ACS APPLIED MATERIALS & INTERFACES

RESEARCH ARTICLE

www.acsami.org

Formation of Defect-Free Latex Films on Porous Fiber Supports

Ryan P. Lively,* Joshua A. Mysona, Ronald R. Chance, and William J. Koros

School of Chemical & Biomolecular Engineering, Georgia Institute of Technology, 778 Atlantic Drive NW, Atlanta, Georgia 30332-0100, United States

Supporting Information

ABSTRACT: We present here the creation of a defect-free polyvinylidene chloride barrier layer on the lumen-side of a hollow fiber sorbent. Hollow fiber sorbents have previously been shown to be promising materials for enabling low-cost CO_2 capture, provided a defect-free lumen-side barrier layer can be created. Film experiments examined the effect of drying rate, latex age, substrate porosity (porous vs nonporous), and substrate hydrophobicity/hydrophilicity. Film studies show that in ideal conditions (i.e., slow drying, fresh latex, and smooth nonporous substrate), a defect-free film can be formed, whereas the other permutations of the variables investigated led to defective films. These results were extended to hollow fiber sorbents, and despite using fresh latex and relatively slow drying conditions, a defective lumen-side layer resulted. XRD and DSC indicate that polyvinylidene chloride latex develops crystallinity over time, thereby inhibiting proper film formation as confirmed by SEM and gas permeation. This and other key additional challenges associated with the porous hollow fiber substrate vs the nonporous flat substrate were overcome. By employing a toluene-vapor saturated drying gas (a swelling solvent for polyvinylidene chloride) a defect-free lumen-side barrier layer was created, as investigated by gas and water vapor permeation.

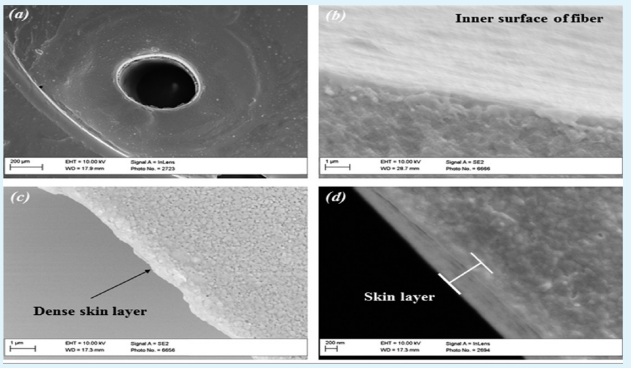

KEYWORDS: barrier layer, polyvinylidene chloride, hollow fiber sorbents, latex age, porous substrate

1. INTRODUCTION

The concentration of CO_2 in the atmosphere has been increasing steadily throughout the Industrial Revolution due primarily to the burning of fossil fuels. This increase is invoked as a significant contributor to global climate change.[1,2] The explosive population growth, requiring ever increasing power generation capacities and large increases in transportation energy usage, is the major cause of growth in CO_2 emissions.[3,4] Prudence dictates that methods for controlling CO_2 emissions be examined and developed.

To reduce or stabilize global CO_2 emissions, a worldwide effort is required, and Pacala and Socolow[5] framed the challenge in terms of seven CO_2 emission "wedges," where each wedge rep resents 50 gigatons of CO_2 avoided over 25 years. Because there is no single "silver bullet" for reducing or even leveling CO_2 emissions, several strategies were considered by these authors, and if all seven wedges start in 2010, global CO_2 emissions will stabilize by 2060. The wedges include measures such as improving the fuel efficiency of vehicles in the fleet from 30 miles per gallon to 60 miles per gallon, building 400 new 1 gigawatt (GW) nuclear power plants, and installing 90% CO_2 capture on 90% of the coal-fired power plant infrastructure. This last wedge has resulted in serious debate, as out of all of the possible CO_2 emission reduction platforms, the capture of CO_2 from power stations is the only strategy that does not result in increased installed generation capacity or increased energy efficiency, but instead energetically taxes the power station because of the added CO_2 capture step. This fact indicates that for CO_2 capture to be a viable route for reducing atmospheric CO_2 concentrations, methods for capturing CO_2 at a minimum parasitic load need to be developed.

A method we recently proposed to reduce CO_2 capture parasitic loads is hollow fiber sorbents,[6,7] which is illustrated in Figure 1. These sorbents achieve the lower energy requirements of adsorption over absorption while mitigating many of the typical processing issues associated with adsorption processes. This goal has been pursued via the creation of a polymer-sorbent composite in the form of a hollow fiber with an impermeable barrier on the inside (lumen side) of the fiber, as seen in Figure 1. By modularizing the fibers and passing the CO_2-laden flue gas on the outside (shell side) of the fibers, we can minimize the total pressure drop across the bed in comparison with a packed bed sorbent system. The hollow fiber morphology, coupled with an ideally impermeable lumen layer, allows for rapid heating and cooling of the thin walled fibers via hot and cold water coursing through the fibers, thus allowing for quicker cycling times and more complete utilization of the

Received: June 19, 2011
Accepted: August 3, 2011
Published: August 03, 2011

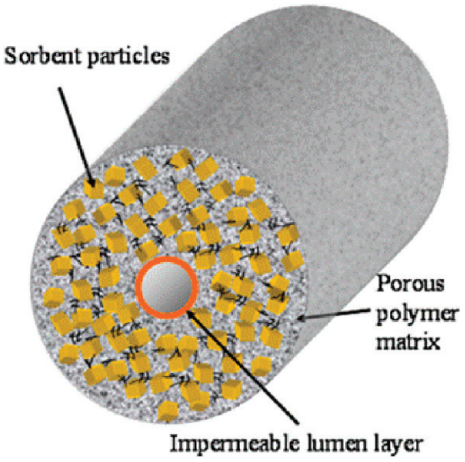

Figure 1. Cross-sectional schematic of a fiber sorbent, illustrating a microporous solid sorbent suspended within a fiber-shaped porous polymer matrix that has an impermeable lumen layer.

sorbents contained with the fiber. Previous work has provided energetic estimates for fiber sorbents[7] that show them to be energetically favorable in comparison to existing and emerging technologies, and has shown that spinning fiber sorbents is a straightforward and consistent process.[6] Up to this point, the creation of a defect-free layer has been elusive,[6] which prevents the fiber sorbents from being used as intended (with cooling water in the bore).[8] This paper illustrates the method for creating a defect-free lumen-side barrier layer from a polymer emulsion—a first in the literature to our knowledge—as well as illustrative experiments that demonstrate the controlling factors of film formation after casting an emulsion-based polymer onto a porous substrate, a topic that is scarcely discussed in the literature.[9,10]

2. BACKGROUND

In the context of this paper, fiber sorbents begin as hollow fiber polymer/zeolite composites spun using a wet phase inversion process[11] at high zeolite-to-polymer loadings. After spinning, the preferred fiber sorbents are finished by post-treatment to create a lumen-side barrier layer using a polyvinylidene dichloride (PVDC) latex. The critically important barrier layer allows for heat transfer fluids to be carried through the bore of the fibers while flue gas flows over the outside of the fibers, transforming the fiber sorbents into "adsorbing heat exchangers[7]". Water is considered as the heat transfer fluid for cooling and hot water or steam as the heat transfer fluid for heating. Fiber sorbents for postcombustion CO_2 capture are intended for use in a rapid thermal swing adsorption (RTSA) cycle, with the rapid cycles allowing minimum device volumes and more effective use of the sorbent.[7]

A convenient way to create the lumen side barrier layer is to use a post-treatment technique based on a polymer latex. A polymer latex is defined as an aqueous colloidal suspension of spherical polymer particles, and is created by an emulsion polymerization. The latex serum (the aqueous dispersion containing the polymer particles) contains electrolytes, surfactants, plasticizers, emulsifiers, initiators and other species.[12] The polymer particles themselves carry surface functionality that serves as a stabilizing agent to allow the aqueous dispersion to stay dispersed. When the latex is cast over a substrate and the aqueous dispersion evaporates, a continuous thin film of polymer is left

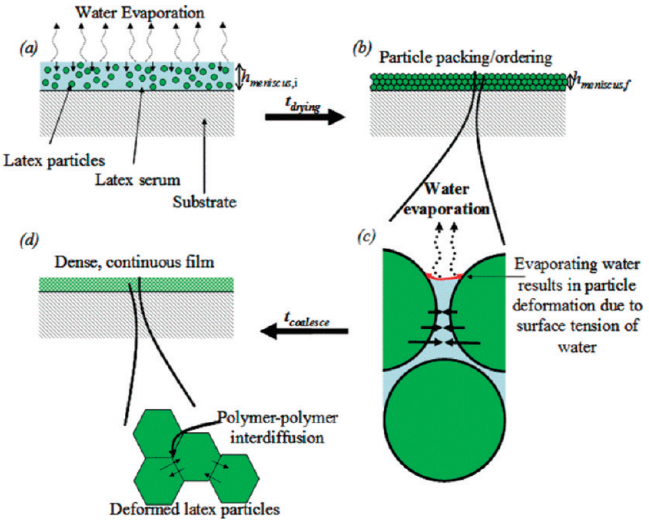

Figure 2. Overview of latex film formation on a dense substrate. (a) After casting, bulk water evaporates slowly from the nascent film, causing the meniscus to shrink (stage I). (b) As the meniscus shrinks, the particles are given ample time to close pack and order as the last of the bulk water evaporates. (c) At a critical polymer concentration, the strong surface tension of the evaporating water pulls the particles close together, finally causing them to deform (stage II). (d) After deformation, the particles (which are now in intimate contact) begin to undergo polymer−polymer interdiffusion to create a dense, continuous film (stage III).

behind. By washing a latex through the bores of the fiber, a polymer layer is deposited on the lumen side of the fiber.

For the lumen layer to be defect-free, the cast latex must form a continuous, dense film. Latex film formation occurs through three main stages: (I) water evaporation/drying, (II) particle deformation, and (III) polymer interdiffusion.[13] One hypothesis is that at a critical polymer concentration, the particles on the outer edges and outer surface of the meniscus will begin to form a dense skin via stage II and III.[16] Finally, the hypothesis posits that the residual water trapped under the forming skin layer must diffuse through the polymer itself[16] or through existing pores between the particles[17] to complete the film formation. Figure 2 gives an overview of this film formation procedure.

2.1. Nascent Film Drying. The drying stage (stage I) occurs initially through a constant loss of water that is similar to simple water evaporation. As the water evaporates, the meniscus of the aqueous colloidal dispersion shrinks, densifying and ordering the polymer particles within;[14] at the same time, the water evaporation rate slows because of the decrease in surface area of the meniscus as well as the increase in polymer concentration.[19]

2.2. Particle Deformation and Polymer−Polymer Diffusion. Directly linked to the water evaporation from the film is the polymer particle deformation. Once the particles are close enough to be in contact, a neck is formed with some radius of curvature (Figure 2c). The interfacial tension between the polymer and water can be estimated using the Young−Laplace equation[18]

$$\Delta p = \frac{2\gamma}{r_p} \quad (1)$$

where γ is the surface tension of the latex serum, and r_p is the radius of the necking region. These interfacial forces begin to deform the polymer particles and allow the process of sintering

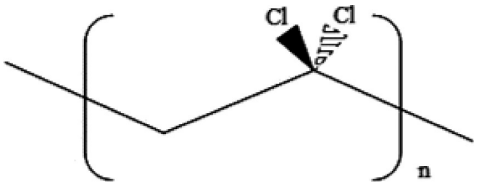

Figure 3. Repeat unit of polyvinylidene chloride.

the particle network into an FCC packing while reptation across the interface proceeds.

As the remaining water in the wet film diffuses out to the atmosphere, a moving front of particle deformation will occur from the bottom of the film toward the top. Once deformed, the polymer particles are believed to form a rhombic dodecahedral structure.[19] Finally, once the polymer particles are deformed and in the rhombic dodecahedral structure, polymer chain interdiffusion (stage III) can occur and "lock in" the deformations, resulting in a dense continuous film.

This paper will first explore the effect drying conditions have on the formation of PVDC films followed by a presentation of the effect of casting substrate on the efficacy of film formation. The effect latex age has on the film formation is then investigated. From here, the results of the film studies are extended toward coating hollow fiber sorbents. The paper then presents the necessity of latex dilution for effective fiber post-treatment as well as the need to not only coat the inside of the fibers, but also the "end-caps" of the fibers. The effect of drying conditions on lumen layer formation is then presented. Finally, a discussion of the results is given, as well as some preliminary hypotheses on the film formation mechanism when casting latexes on porous supports.

3. MATERIALS AND METHODS

Hollow fiber sorbents used in this work have been previously spun[6] using the wet-quench spinning process.[11] The fiber sorbent is a matrix of cellulose acetate (CA) and zeolite 13X with a dry zeolite loading of 75 wt %. The fibers are porous throughout, and are approximately 1100 μm in diameter, with a bore diameter of approximately 320 μm. Polyvinylidene chloride (PVDC) was chosen as the barrier layer polymer in this work. PVDC latex for application in the lumen layer was supplied by SolVin Chemicals (Northwich, UK), batch name XB 202. According to SolVin Chemicals, the PVDC latex is 55% by volume solids, the latex serum is anionic with a pH of 1.5. Finally, this batch of PVDC latex has copolymer components of polymethylmethacrylate (PMMA) to improve the temperature resistance of the polymer. PVDC was chosen for its remarkable properties as a barrier, and the structure of PVDC and its gas permeabilities can be seen in Figure 3 and Table 1, respectively.

3.1. Barrier Layer Formation. Creation of the lumen layer via a post-treatment method is straightforward in principle. By using a latex, the need for an organic solvent is eliminated and allows for multiple "washes" if needed, followed by a nitrogen sweep step to remove the excess serum and dry the nascent barrier layer. This method also has the advantage of being quite tunable: latex concentration, drying gas humidity, length and number of washes, and pressure of the feed latex are the principal parameters that can be varied.

The fiber sorbents were assembled into standard shell and tube modules with a length of 15−24 cm[8]. Fiber modules were attached to the post-treatment system and flowing humid N_2 presaturated the pores of the fiber with water vapor. Fibers were then post-treated by flowing latex at varying levels of dilution (between 10 vol % latex in H_2O and pure latex) through the bores of the fiber at 600 mL/h-fiber with 30 mL of fluid using a 1 L ISCO syringe pump while the fiber ends were submerged in a hexane bath to prevent any rapid latex drying and subsequent fiber plugging at the tips of the fibers. The layer was then dried in several different ways, which are tabulated in Table 2.

Table 1. Permeabilities of PVDC to Some Common Gases[21a]

	P_{H2O}	P_{CO2}	P_{N2}	P_{He}	P_{O2}
polyvinylidene chloride	3.0	0.012	0.001	0.066	0.002

[a] All values in Barrers: 1 Barrer = 1×10^{-10} [cc(STP) cm]/[cm^2 s cm Hg].

Table 2. Summary of Drying Procedures

drying method	drying procedure
dry	6 h dry nitrogen, 15 h 71 °C vacuum
wet	6 h saturated nitrogen, 15 h 71 °C vacuum
graded	6 h saturated nitrogen, 15 h 25%RH at 25 °C
toluene-assisted	6 h water-and-toluene-saturated nitrogen, 15 h 25% RH at 25 °C

"Dry" drying used dry nitrogen immediately after the latex deposition to dry the nascent latex film followed by vacuum drying at 71 °C. 71 °C was chosen as a sufficiently high temperature to remove all of the excess water in the samples (under vacuum) yet low enough that any temperature-induced effects could be neglected. "Wet" drying used water-vapor-saturated N_2 to dry the latex film followed by vacuum drying at 71 °C. "Graded" drying again uses wet N_2 (N_2 sparged through a water column) to initially dry the layer followed by 15 h of ambient air drying. "Toluene-assisted" drying uses toluene-saturated and water-saturated N_2 to dry the fibers before 15 h of ambient air drying. The module was then flipped over and the experiment was repeated. Finally, PVDC latex of two different ages were used—2 years old and fresh latex.

3.2. Formation of Dense Films from PVDC Latex. PVDC film formation was studied by casting from the latex (old and new) on a variety of substrates. Cellulose acetate/13X composite films were formed by casting excess polymer dope from the spinning experiments onto a glass plate and immediately quenching into DI H_2O followed by the standard dehydration techniques. Other substrates studied were smooth glass, etched glass, porous nylon 6,6 (Whatman International Ltd., Maidstone, England, 0.2 μm pore), and porous PVP-free polycarbonate (Poretics Corporation, Livermore, CA, 0.1 μm pore). The glass substrates were cleaned with acetone and soap water before use, whereas the porous substrates were used as-is. The substrates were placed on a leveling base (Paul Gardener Company, Pompano Beach, FL) and set to be perfectly level using a bubble leveler. The substrate and leveling agent were placed into a glovebag (Aldrich, Milwaukee, WI) along with a doctor knife (Paul Gardener Company, Pompano Beach, FL), sealed off and filled with the appropriate atmosphere (dry N_2 or wet N_2) and purged three times with that atmosphere. The casting knife was then placed at one end of the plate as ~4 mL of latex was poured onto the substrate. Finally, the knife was drawn across the substrate to evenly distribute the latex. After the same amount of drying time that the fibers were given, the films were removed from the bag and either sent to the vacuum oven for 71 °C drying or allowed to dry in ambient air for 15 h.

3.3. Evaluation of PVDC Coatings. *3.3.1. Gas Permeation.* After the fiber sorbents were post-treated, the gas transport properties of the bare fiber sorbents were probed via N_2/He permeation using an isobaric system (constant pressure, variable volume) with bore-side feed

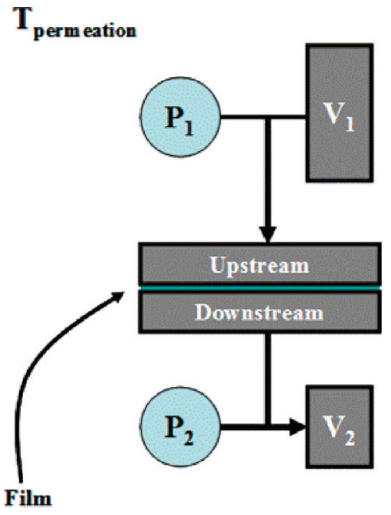

Figure 4. Simplified schematic of an isochoric permeation system. P_1 represents the upstream pressure transducer, while V_1 represents the upstream volume. P_2 and V_2 represent the downstream pressure transducer and volume, respectively. Typically, $V_1 \gg V_2$. The system is held at constant temperature, $T_{permeation}$.

pressures of 20−100 psig at 35 °C. This gas pair was chosen because of the different selectivities for bulk and Knudsen transport (1 and 2.67, respectively), and because of the fact that both of these gases are inert toward CA and PVDC. Gas flow on the shell-side of the module was measured using a bubble flow meter every 45 min until the readings were within 5% of the previous reading. The volumetric flow rate can then be readily converted to molar flow rate, which in combination with the barrier layer inner diameter, allows the permeance of the layer to be calculated. Permeance refers to a pressure normalized flux, which does not normalize the flux for the effective thickness, since this thickness can be difficult to determine in asymmetric and porous coated surfaces. The units of permeance are GPUs, where 1 GPU = 1×10^{-6} [cc(STP)]/[cm^2 s cm Hg].

The PVDC films were first tested using an isobaric system in the same fashion as described above. If the films were defect-free, they were then moved to a constant volume—or isochoric—system. The PVDC films were masked into a custom built permeation cell comprised of two stainless steel plates with a sintered steel disk placed on the bottom plate to serve as a support for the film.[22] The cell was then installed into a constant temperature permeation box by attaching it to a feed and permeate volume. A simple schematic is given in Figure 4.[23]

A constant feed pressure was supplied to the upstream volume, while the downstream volume was kept under high vacuum. Leak rates in the system were monitored, and were usually on the order of 1×10^{-6} to 1×10^{-7} Torr/s. A permeation experiment began when the downstream vacuum was closed, and the upstream feed valve was opened. The pressure rise in the downstream volume was monitored via a 10 Torr transducer (MKS Instruments, Andover, MA). Knowledge of the downstream volume as well as the pressure rise in the volume allows for calculation of the molar flux of gas across the PVDC film.

3.3.2. Water permeation. Water permeability of the PVDC lumen layer was tested by attaching a backpressure regulator to the end of the fiber module and pressurizing liquid water in the bore of the fiber via a 100 mL ISCO pump to 40 psig. While water was pressurized in the bore, nitrogen at 300 sccm flowed on the shell side of the module and was sent to a Pfeiffer Vacuum QMS 200 Omnistar Mass Spectrometer. From these data, the water vapor content in the nitrogen could be found, allowing for the calculation of the molar flow rate of water permeating through the fiber sorbents. The experiments were stopped after 5 days on line because of the excessive use of nitrogen required. These experiments were conducted only on PVDC layers that were defect-free in order to prevent flooding the mass spectrometer with water.

3.4. Supporting Experiments. *3.4.1. Scanning Electron Microscopy.* Scanning electron microscopy (SEM) was used to evaluate the fiber and film samples. Solvent exchanged fibers were soaked in hexane for 2 min, transferred to liquid N_2, and sheared in half using two fine point tweezers. This procedure ensured sharp fiber breaks, and the fibers were then sputter-coated with a 10−20 nm thick gold coating (Model P−S1, ISI, Mountain View, CA), and transferred to a high resolution Field Emission Scanning Electron Microscope, Leo 1550 (Leo Electron Microscopy, Cambridge, UK). The same procedure was repeated for the PVDC films.

3.4.2. X-ray Diffraction. X-ray diffraction was used to search for any crystallinity in the PVDC films. The data in this study were collected via Ni-filtered Cu Kα radiation on a PanAlytical X'Pert PRO machine. The film samples were stacked and supported with a clip into the sample holder. A step-scanning protocol was used, where 0.02° 2θ steps were taken from 5 to 70° 2θ at 1 s per step. θ is the Bragg angle.

3.4.3. Differential Scanning Calorimetry. Differential scanning calorimetry (DSC) was employed to demonstrate the difference in morphology between aged and fresh PVDC films cast on smooth glass. It is well-known that the presence of crystallinity increases glass transition temperature compared to noncrystalline sample. The instrument for this characterization was model Q800 from TA Instruments. Glass transition temperature was determined from the first scan by taking the half height of heat increment. Each run was made at 10 °C/min from −50 to 170 °C. Nitrogen flow at 50 mL/min was maintained to prevent any oxidation of polymer during run.

4. RESULTS

4.1. Film Studies. The background section discussed some general hypotheses regarding formation of dense films from latexes on smooth, dense, and continuous substrates. While the literature on this topic has grown substantially in the past twenty years,[24] very few attempts have been made to characterize or understand the film formation properties when the latex is cast onto a porous substrate.[9,10] Further complicating this case for fiber sorbent post-treatment applications, the PVDC latex must be forced through a 300−400 μm hollow fiber bore while in contact with a highly porous, rough, hydrophilic, inorganic−organic hybrid material, and then followed by a forced convection drying via a gas sweep through the bores of the fibers. This introduces many new nonidealities into the film formation process and the resulting film can have defects that range from the macroscopic scale down to the nanoscopic scale. For an effective barrier, the layer must be nearly molecularly perfect, with very few defects. Because eof the myriad of nonidealities that have been introduced by casting the layer onto the cellulose acetate/13X fiber sorbent matrix, several film-based experiments were performed to isolate the most relevant factors impacting the film formation process.

One of the main issues associated with a lumen-side fiber sorbent post-treatment using an aqueous latex is the capillary forces that arise as a result of the porous substructure. These capillary forces are caused by the latex being able to wet the inner surface; once the latex wets the inner surface, the liquid will attempt to minimize its free energy by filling the pores of the fiber.[25] The pore-filling action removes latex serum from the latex, most likely inhibiting defect-free film formation (discussed later in the Discussion section). To investigate this capillarity effect, latex films were cast on continuous glass plates (control),

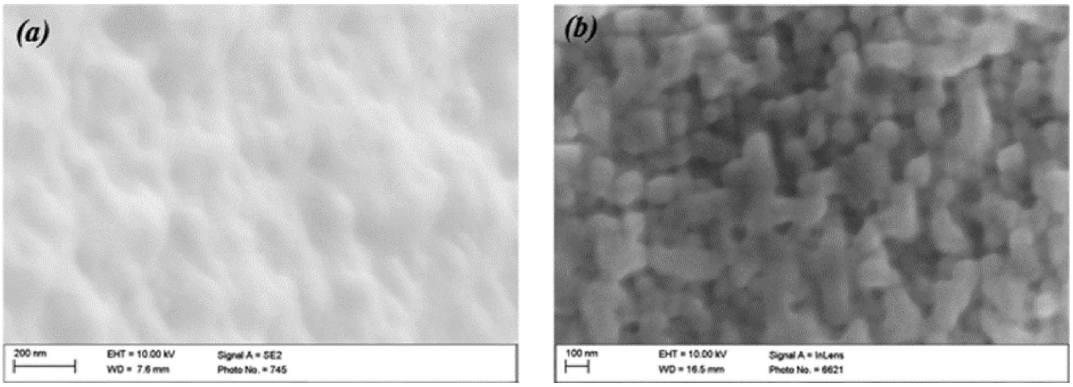

Figure 5. High-magnification SEM images of "crack-free" areas of PVDC films cast using the "wet" drying method. (a) PVDC films cast from the fresh PVDC latex show a lumpy surface with well-adhered, deformed PVDC particles. (b) PVDC films cast from the aged latex show a globular structure with poor particle deformation and intercalation.

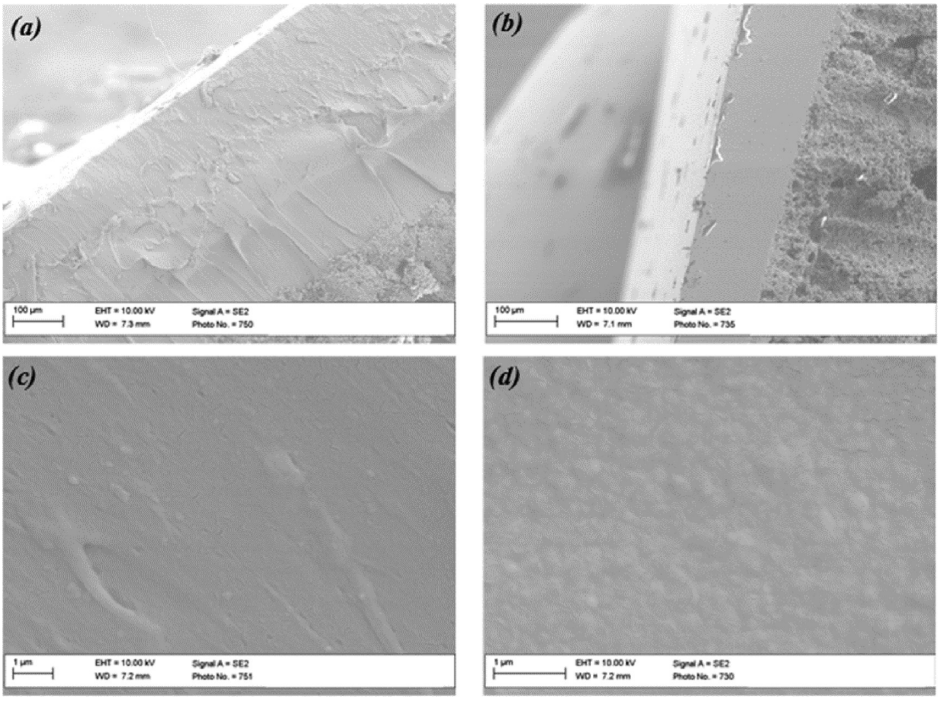

Figure 6. PVDC films cast onto a cellulose acetate/13 X support using the "graded" drying mode. (a) Film cast from new PVDC latex shows good adhesion to CA support. (b) Film cast from aged PVDC latex shows good adhesion to CA support, though some cratering is observed in the cross section of the film. (c) Enhanced magnification of PVDC film from the fresh latex shows a continuous structure with no globular particles detected. (d) Enhanced magnification of PVDC film from the aged latex shows a continuous structure with slightly globular particles detected.

porous hydrophobic substrates, porous hydrophilic substrates, and cellulose acetate/13X films. Another nonideality is the lack of smoothness of the inner surface of the fiber. If there are any large discontinuities in the surface, such as a crevice, the ability of the nascent film to form a continuous layer will be undermined by the inability of the film to coalesce at the discontinuity, an example of which is illustrated in Figure S1 in the Supporting Information. This effect was investigated by casting films on a smooth glass plate (control) and a finely etched glass plate, where the etches represent large discontinuities in the film.

Once the lumen layer has been successfully cast onto the inner surface of the fiber, the layer must undergo drying. Unlike conventional flat sheet drying, free convection/evaporation drying is difficult to achieve within fiber sorbents, as the remaining latex held within the bore needs to be evacuated after the post-treatment. Therefore, a forced convection gas sweep is used to dry the lumen layer, which—depending on the water vapor content of the gas—has the possibility to be a much more accelerated drying rate than simple free evaporation at ambient conditions. To investigate this effect, we chose three drying conditions for PVDC films cast onto cellulose acetate/13X films (Table 2): completely dry nitrogen followed by 71 °C vacuum ("dry" mode), water-vapor-saturated N_2 followed by 71 °C vacuum ("wet" mode), and water-vapor-saturated N_2 followed by drying at ambient conditions ("graded" mode). Finally, the latex age can have a large impact on the continuity of the final

Table 3. Effect of Drying Rate on PVDC Film Formation (CA/13X substrate)[a]

	drying method					
	"dry"		"wet"		"graded"	
latex sample	helium permeance (GPU)	He/N_2 selectivity	helium permeance (GPU)	He/N_2 selectivity	helium permeance (GPU)	He/N_2 selectivity
2-year aged	$4.8 \pm 0.11 \times 10^5$	1.76 ± 0.05	$5.3 \pm 0.28 \times 10^5$	2.15 ± 0.15	54.7 ± 0.4	1.63 ± 0.05
fresh	$6.9 \pm 0.15 \times 10^5$	2.5 ± 0.4	$2.2 \pm 0.19 \times 10^5$	2.2 ± 0.03	5.6 ± 0.4	1.87 ± 0.1

[a] Standard deviation is the result of three permeation experiments on three separate films. $T = 35°C$, feed pressure of 10 psig used for highly defective films ($>1 \times 10^4$ GPU), 100 psig for slightly defective films (<1000 GPU).

film. To test this effect, the substrate and drying rate experiments were repeated for fresh PVDC latex as well as PVDC latex that had been stored in our laboratory for 2 years under ambient (dark) conditions.

4.1.1. Effect of Drying Condition. PVDC latex was cast onto cellulose acetate/13X mixed matrix films and dried several different ways, as mentioned above. During the wet phase of the film casting, no obvious changes such as bubbling or skin formation were observed in the nascent films. In the "wet" drying mode the film was moved to a vacuum oven to remove excess water which resulted in very rapid film formation. This rapid film formation resulted in large stress fractures for the aged latex films and bubbles and boils in the fresh latex film (Figure S2 in the Supporting Information). When the films were dried in a dry glovebag ("dry" mode) a thin cloudy skin layer could be observed on the outer surface of the nascent film. However, once the film was moved to the vacuum oven, rapid film formation again occurred, resulting in large stress fractures and bubbles in the aged and fresh latex films, respectively. The absence of bubbling in the aged latex films is especially interesting, as it likely indicates that the latex loses some volatile component over time. One hypothesis is that the latex loses a volatile "leveling agent"; this leveling agent serves to reduce the T_g of the PVDC particles, thereby allowing them to more easily coalesce with nearby particles.[25] Finally, films dried with the "graded" drying protocol were found to form an amber colored and crack-free film after approximately 15 h drying at ambient conditions.

Figure S2 shows SEM images of the aged and new latex films cast onto the cellulose acetate/13X support dried via the "wet" and "dry" drying method. The figure illustrates the bubbling and cracking effects that were visually observed during the film formation experiments. Closer examination of the noncracked film areas indicates the presence of well-formed, dense areas of PVDC when the new latex is used, whereas porous, poorly formed films are found when the aged latex is used, as seen in Figure 5. This likely indicates that, at least in the case of the new PVDC, a continuous film forms correctly during the rapid drying, but the necessity for stress relaxation causes it to crack.

When the drying rate is markedly slowed via the "graded" drying mode, the film was found to form a dense, level coating on top of the cellulose acetate/13X matrix, as seen in Figure 6. The coating appears to be well-adhered to the cellulose acetate/13X matrix, and no cracks or large crazes could be detected in the cross-sectional SEM images. However, the aged latex film was found to have sizable craters found in the cross-sectional images (Figure 6b). As can be seen in Figure 6c, the films cast from the new latex yield a dense PVDC layer with no PVDC globules visible, indicating that the film likely formed correctly. In the case of the films cast from the aged PVDC, a dense layer is also observed; however, the PVDC globules are still slightly visible, but appear to be well adhered to each other. From SEM images alone, the "graded" drying method is clearly preferred for drying the nascent PVDC films. Of course, SEM images alone cannot show nanoscopic defects that a gas molecule might "see". Therefore, helium and nitrogen permeation experiments were performed on these six films to elucidate the true extent of proper film formation.

Table 3 shows the results from the helium and nitrogen permeation experiments. As expected from both visual observations and SEM images, the films dried via the "wet" and "dry" mode are completely defective, yielding permeances essentially the same as the support material permeance (the support material has a helium permeance of approximately 70,000 GPU). The He/N_2 selectivity through the films is close to Knudsen selectivity (2.6 for helium/nitrogen), though a bulk selectivity contribution is clearly present. Due to the large PVDC cracks, the dominating resistance to permeation is most likely the CA/13X film. The films dried in the "graded" mode—which were visually the most promising—yielded significantly lower permeances than the defective films. It is interesting to note that the 2-year aged latex yields a helium permeance of ~55 GPUs, whereas the new latex yields a helium permeance of ~5.5 GPUs. A Knudsen selectivity of 2.6 is expected if the pore radius is a tenth of the mean free path of either helium or nitrogen, and bulk selectivities are expected if the pore radius is an order of magnitude larger than the mean free path.

The selectivities observed in these experiments are near 1 (bulk) and 2.65 (Knudsen), indicating that there exists a porous pathway through the film that has a pore radius that allows for both Knudsen and bulk diffusion to contribute. As judged by the higher selectivities and lower permeances of the films cast from the new latex, perhaps the pores that form are fewer and perhaps smaller compared to the aged latex, and the pathway through the film is a more tortuous one. This concept of a "porous" barrier layer is important for the discussion of the film formation mechanism, which is discussed later. The "graded" drying mode and the use of fresh latex are clearly preferred for formation of the barrier layer, though there is much work required to optimize this drying procedure to result in "defect-free" films cast onto porous supports.

4.1.2. Effect of Substrate. Once a drying rate was established that allowed for adequate film formation (a 1×10^5 reduction in permeance when compared to the uncoated substrate) on cellulose acetate/13X substrates, the effect of the substrate on the latex film formation properties was studied. Smooth glass (control) and etched glass substrates were used to investigate film formation mechanisms in ideal, nonporous conditions, while porous nylon 6,6 films were used to test hydrophilic porous

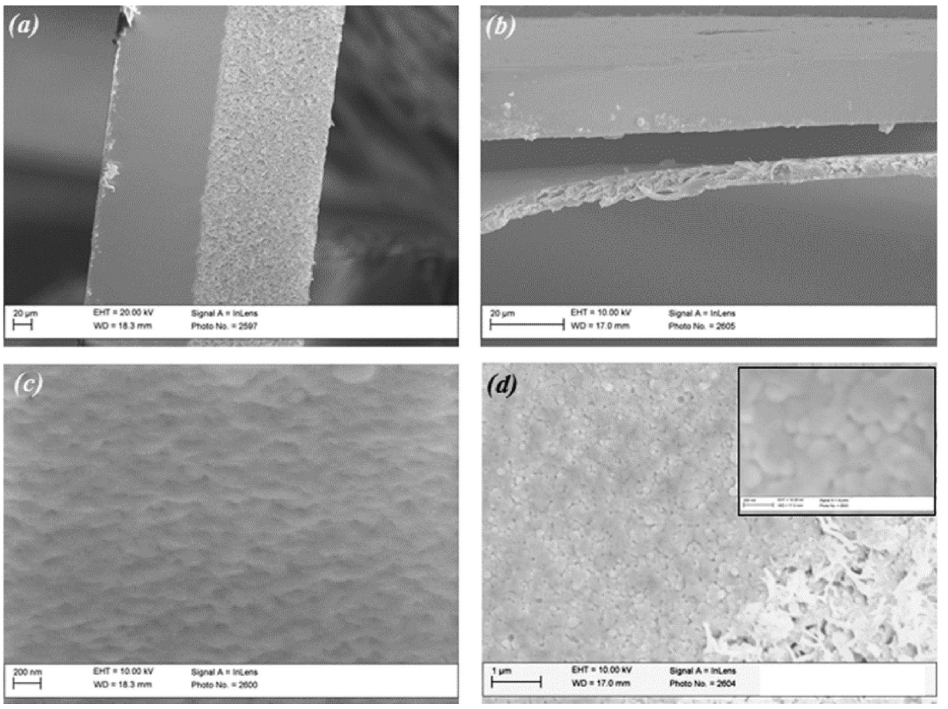

Figure 7. SEM images of aged and fresh PVDC latex cast onto nylon 6,6 and PVP-free polycarbonate substrates. (a) PVDC (fresh latex) film well adhered to nylon 6,6 substrate. (b) PVDC (aged latex) delaminated from polycarbonate substrate. (c) High-magnification image of PVDC from fresh latex cast onto nylon substrate showing partially deformed, intercalated particles. (d) High-magnification image of PVDC from aged latex cast onto nylon substrate showing deformed particles that are poorly intercalated. Inset clearly shows lack of particle intercalation.

substrates, and porous PVP-free polycarbonate films were used to test hydrophobic porous substrates. Fresh and aged latex samples were cast onto these four substrates and were dried using the "graded" drying mode investigated in the previous section. For the glass substrates, a water meniscus was observed on the glass plate that slowly receded as the film dried with a milky center and clear edges. Once dried, the new latex formed a clear and highly flexible film, not unlike common household Saran. Though films cast on the etched glass had the imprint of the etches formed into the film, these films were just as flexible. However, the aged latex formed an amber colored film that was highly brittle; again, the shape of the etches on the plate were imprinted into the film. One-inch strips of the films from the aged latex/smooth glass were able to be bent approximately 130° before breaking, whereas one inch strips from the aged latex/etched glass were only able to be bent approximately 45° before breaking (for films of the same thickness). Interestingly, the breaks in the etched glass film almost always occurred at the etch imprints of the film where stress concentration points (or lack of film coalescence) exist. The new latex films were not able to be broken via simple bending tests.

Films cast onto the hydrophobic polycarbonate substrate were observed to poorly coat the substrate with the PVDC latex pooling together above the substrate, leaving parts of the substrate uncoated. This was confirmed once the nascent latex was dried: films were poorly formed, brittle, and not adhered to the polycarbonate substrate. This was observed in both fresh and aged latexes. Although the hydrophobic substrates had incomplete coatings, PVDC films cast onto the hydrophilic nylon substrates were found to make smooth and even coatings from the fresh latex. SEM images of the films cast onto the hydrophilic substrate show a well-adhered, even coating (Figure 7a), whereas the films cast onto the hydrophobic substrate exhibit delamination between the PVDC and PC layers (Figure 7b). Upon closer magnification, the fresh PVDC cast onto the nylon substrate showed partial particle deformation and particle intercalation (Figure 7c), although a porous structure was still obtained. The aged PVDC cast onto the nylon substrate showed particle deformation, yet seemingly poor polymer−polymer interdiffusion (Figure 7d and inset, respectively).

SEM images in Figure 8 of the smooth and etched glass PVDC films reveal a marked difference between the aged and new laticies. The PVDC films from the aged latex were found to exhibit globular morphology in the cross-sectional images for both smooth and etched glass substrates (not shown). Further magnification reveals the individual PVDC particles packed together, with only slight intercalation between the particles observed (Figure 8a). The face of the film cast on the etched glass substrate has large discontinuities corresponding to the etch imprints (Figure 8b), with large cracks clearly present. The films cast onto the smooth glass do not exhibit this phenomenon. The films cast from the fresh latex did not exhibit this severe of a globular structure in the cross-sectional images. Upon further magnification a "lumpy" surface is still exhibited indicating that perhaps the PVDC particles have not completely intercalated (Figure 8c). Finally the outer edge of the film was found to be quite dense, smooth, and free of the aforementioned "lumpy" surface (Figure 8d). Furthermore, there was no observable discontinuities occurring at the etch lines for the fresh PVDC film cast on the etched glass substrate (not shown).

Of course, SEM images do not completely reveal the perfection of the barrier polymer. To that end, helium and nitrogen permeation experiments were again used to probe the PVDC films. Table 4 summarizes the permeation results of the films cast

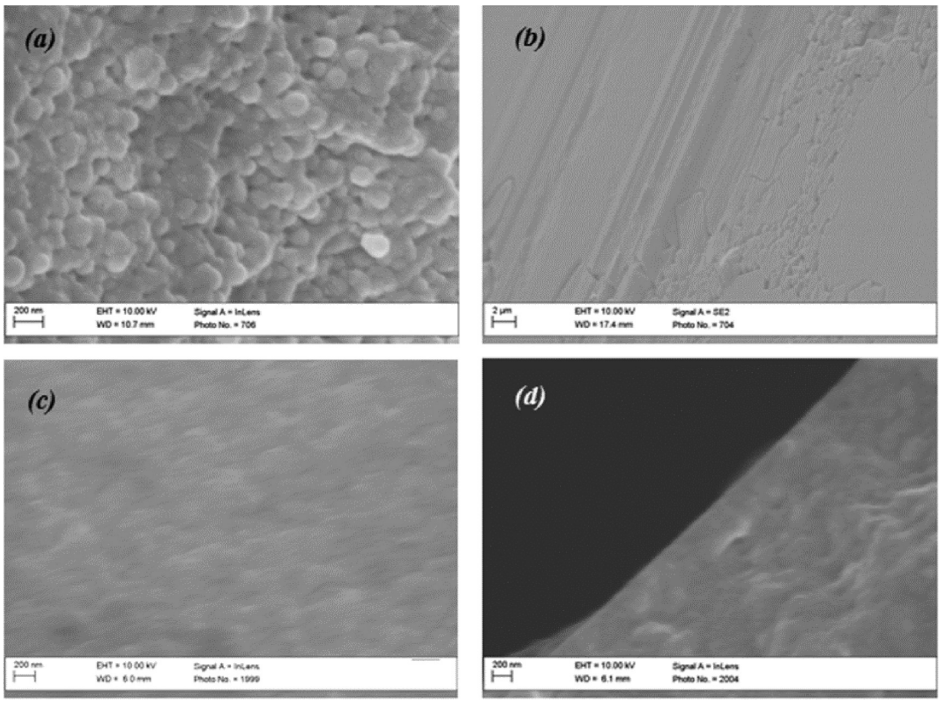

Figure 8. SEM images of PVDC films cast onto smooth and etched glass substrates. (a) Aged latex cast onto smooth glass substrate. (b) Aged latex cast onto etched glass substrate. (c) Fresh latex cast onto smooth glass substrate. (d) Fresh latex cast onto etched glass substrate.

Table 4. Effect of Substrate on PVDC Film Formation ("graded" drying)[a]

	substrate			
	PVP-free porous polycarbonate		porous nylon 6,6	
latex sample	helium permeance (GPU)	He/N_2 selectivity	helium permeance (GPU)	He/N_2 selectivity
2-year aged	$3.5 \times 10^4 \pm 0.01$	2.28 ± 0.02	121 ± 0.28	1.1 ± 0.05
fresh	$1.3 \times 10^4 \pm 0.05$	2.2 ± 0.05	0.41 ± 0.02	1.2 ± 0.13
	smooth glass		etched glass	
latex sample	helium permeance (GPU)	He/N_2 selectivity	helium permeance (GPU)	He/N_2 selectivity
2-year aged				
fresh	1×10^{-4}	∞	1×10^{-4}	∞

[a] Standard deviation represents three permeation experiments on three separate films. $T = 35°C$, feed pressure of 10 psig used for highly defective films ($>1 \times 10^4$ GPU), 100 psig for slightly defective and defect-free films (<1000 GPU). Nitrogen permeance for defect-free films were too low to measure. Aged latex films cast onto glass were too brittle to test.

onto varying substrates. The films cast onto the hydrophobic polycarbonate films were, as expected, severely defective, yielding high fluxes through the film. PVDC films cast from the aged latex onto the porous nylon substrate were also highly defective, as confirmed by the SEM images in Figure 7. Most interestingly, the films from the fresh PVDC latex cast onto the hydrophilic nylon exhibit very low helium permeance of 0.4 GPU, as opposed to the 5.6 GPU permeance exhibited by the cellulose acetate/13X films cast from the same latex (the films were approximately the same thickness). The images in Figure 7 suggest that while the fresh latex exhibited good particle intercalation, the aged latex did not, perhaps explaining the large difference in helium permeance that was observed. The near-bulk selectivity observed likely indicates the presence of large pores in the PVDC film. If the defects through the film have pore sizes that are larger than 210 nm (an order of magnitude more than the helium mean free path at 100 psig), then bulk selectivities would be expected. The films cast from the aged latex onto the glass substrates—both smooth and etched—were too brittle to mask the films into the permeation cells; films that were able to be successfully masked were fractured by the low gas pressures used in these experiments.

Finally, for the films cast from the fresh PVDC latex onto the glass substrates, permeances were too low to be measured on the isobaric system. These films were installed into the isochoric system and exhibited extremely low helium permeances of approximately 1×10^{-4} GPU; nitrogen fluxes were much lower than the capabilities of the permeation system (the nitrogen

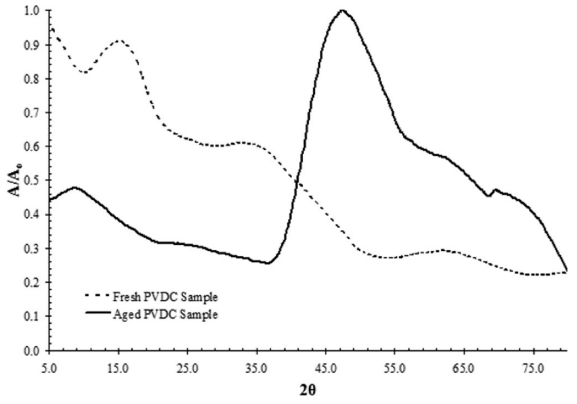

Figure 9. XRD plot of PVDC sample fresh from supplier (dotted line) and PVDC sample aged for 2 years (solid line).

permeation experiments yielded the same results as a typical leak test). This indicates that given an ideal (or even slightly nonideal, as in the case of the etched glass) substrate and a reasonable set of drying conditions ("graded" drying mode), the fresh PVDC latex performs as desired for this application.

4.1.3. Effect of Latex Age. As observed in the previous sections, the age of the latex has a marked effect on the film formation properties and subsequent permeation results. To investigate this, the two latex samples cast onto the smooth glass substrate (the control substrate) using the "graded" drying mode were analyzed via XRD and DSC. XRD results, in Figure 9, show a typically amorphous diffraction pattern for the film from the fresh PVDC latex, as expected. The films cast from the aged latex show a distinct shift in the diffraction pattern toward high angles.

Using Bragg's Law[26]

$$n\lambda = 2d\sin\theta \quad (2)$$

the d-spacing of the aged PVDC sample is estimated to be approximately 1.6 Å. Although there is a significant amount of spread in the diffraction pattern, this indicates that there exists a small fraction of crystallinity[27] in the aged PVDC.

DSC further confirms this inference, as seen in Figure S3 in the Supporting Information, where the fresh latex sample exhibits a small cold crystallization peak (at ~75 °C) while the aged sample does not exhibit this peak. This implies that the fresh sample has more amorphous phase than the aged sample (or, the aged sample possesses more crystallinity than the fresh sample).[28] Furthermore, the T_g of the aged latex is shifted higher (+ 5−7 °C higher T_g) than that of the fresh latex, reflecting the presence of additional crystallinity in the aged latex. The effect of this crystallinity will be discussed in the Discussion section.

4.2. Development of PVDC Lumen Layer, Fibers. The film experiments were conducted to gain insight into the latex film formation mechanism on porous supports, with the ultimate goal being extension to lumen-side coating of fiber sorbents. Fiber sorbents were potted into 8 in., one-fiber modules. The fibers were dried in "dry," "wet," "graded," and "toluene-assisted" modes. For the fibers to be tested in RTSA mode, the lumen side PVDC layer must be defect-free. Any defects in the lumen layer will allow water to rapidly bypass the barrier layer, reducing the CO_2 capacity of the zeolite 13X contained within the cellulose acetate support.

4.2.1. Necessity for Dilution of Latex. Initial experiments attempted to post-treat the as-received PVDC latex directly onto

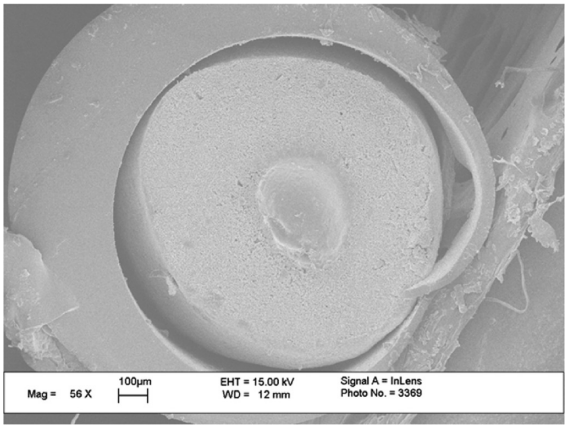

Figure 10. SEM image of a PVDC-plugged fiber as a result of insufficient latex dilution.

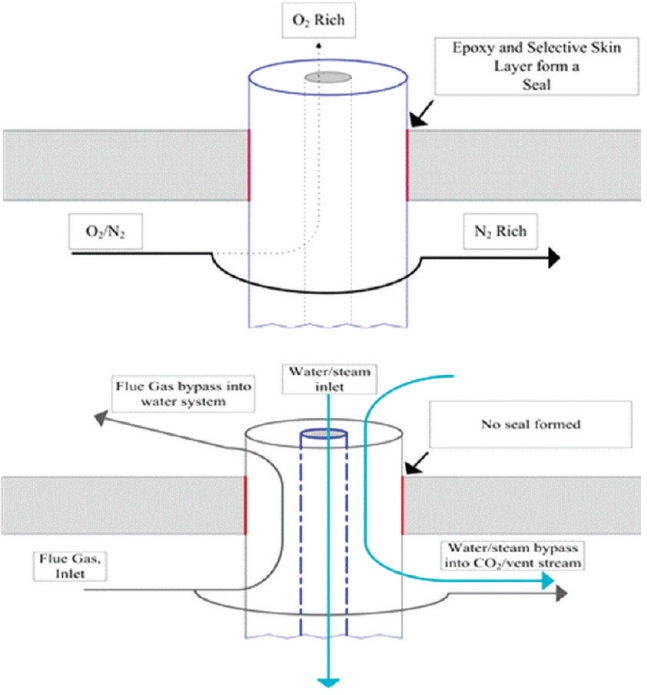

Figure 11. Illustration of lumen layer bypass. (Top) Typical potting of a hollow fiber membrane separates the feed and permeate side. (Bottom) Typical potting in a hollow fiber sorbent does not effectively separate the feed and permeate sides of the fiber.

the lumen side of the fiber. Unfortunately, this always resulted in a solid plug of latex forming in the middle of the fibers, effectively blocking the bore of the fiber, as seen in Figure 10. Presaturating the pores in the fibers with wet nitrogen was found to reduce the plugging that occurred in the fiber bores. However, the incidence of fiber plugs was still unacceptably high. Deionized water was used to dilute the latex, as well as to decrease the viscosity of the latex. Furthermore, the extra water allows the latex dispersion to remain stable in the face of the strong capillary forces exhibited by the porous support, which is discussed at length in the discussion section. At 40 vol % H_2O/60 vol % PVDC latex, the latex post-treatment process was found to never plug the fiber sorbents with latex. This diluted latex was used for all subsequent experiments.

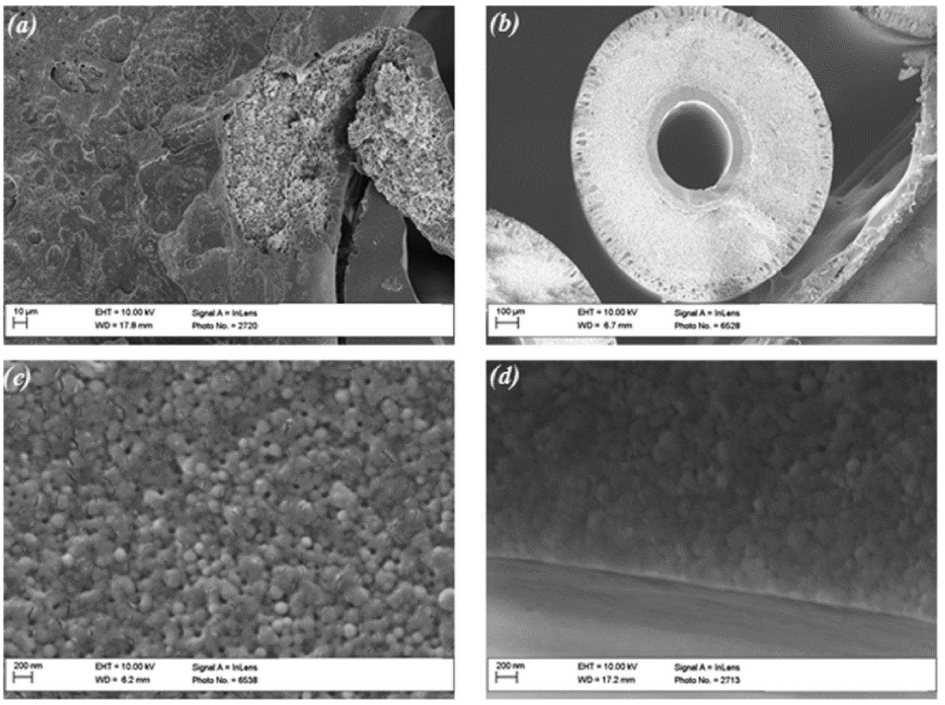

Figure 12. SEM images for PVDC-coated fiber sorbents. (a) Face-seal of fiber sorbent showing matted PVDC structure as well as large defect, revealing the CA/13X structure underneath. (b) Fiber sorbent with PVDC lumen layer. (c) High magnification of PVDC layer cast from aged latex. (d) High magnification of PVDC layer cast from fresh latex.

Table 5. Permeation Results for CA/13X/PVDC Fiber Sorbents[a]

	drying method					
	"dry"		"wet"		"graded"	
latex sample	helium permeance (GPU)	He/N_2 selectivity	helium permeance (GPU)	He/N_2 selectivity	helium permeance (GPU)	He/N_2 aelectivity
2-year aged	63.8 ± 0.9	2.1 ± 0.03	6.8 ± 0.55	1.94 ± 0.26	3.26 ± 0.02	2.8 ± 0.27
fresh	41.9 ± 1.8	2.2 ± 0.19	1.45 ± 0.01	1.98 ± 0.19	0.21 ± 0.01	2.8 ± 0.20

[a] Standard deviation refers to three permeation experiments on three separate fibers. $T = 35°C$, test pressures = 20 psig.

The pressure drop through the fiber module was monitored during the post-treatment experiments. Upon insufficient latex dilution, an immovable plug of polymer was found to form in the bores of the fibers (Figure 10, which permanently sealed the bore and resulted in pressures that exceeded our pumping systems capabilities (>1000 psig). At the appropriate latex dilution, the pressure drop through the fiber module was found to be approximately 105 psi/ft, which is close to a simple Hagen−Poiseuille estimate of the pressure drop. As the latex dilution went beyond the necessary dilution, the pressure drop decreased. At 10 vol % latex in water, the pressure drop was approximately 26.5 psi/ft.

4.2.2. Lumen Layer Bypass. An additional issue that had to be overcome with fiber sorbents involved lumen layer bypass. In a typical selective hollow fiber membrane, the outer selective skin seals against the potting material (typically an epoxy[29]), thereby forcing feed streams to pass through the selective portion of the fiber (Figure 11, top). In a fiber sorbent, however, with the barrier layer on the interior of the fiber, no such seal exists between the epoxy and the lumen-side barrier layer. As such, water and steam that are introduced on the bore-side can bypass through the highly permeable core structure of the fiber into the shell-side of the manifold. Furthermore, flue gas from the shell-side feed could escape into the water and steam systems (Figure 11, bottom). This problem, if not remedied, would render the RTSA system ineffective. From a laboratory perspective, if lumen layer bypass is not addressed, the true permeance of the barrier layer will never be known, as the defective end-caps would dominate permeation through the fiber sorbent. To counter this, a simple method of "capping" the fibers at the potting seals was developed. During the post-treatment experiment, capillary forces present at the face of the fiber pull the latex into the top face of the fiber (or the latex feed side of the fiber) while the bottom face of the fiber (or the latex effluent side of the fiber) is submerged in hexane. The subsequent gas drying step must be carefully chosen to assist in the formation of a defect-free cap layer as well as a defect-free lumen layer.

4.2.3. Effect of Drying Rate and Latex Age. 4.2.3.1. "Dry" Mode. Fibers dried using the "dry" mode were found to be the most defective; SEM images in Figure 12 show the fiber lumen layer as well as a cracked fiber face that exhibited matted, poorly formed PVDC; likely due to rapid stress-relaxation at the face of

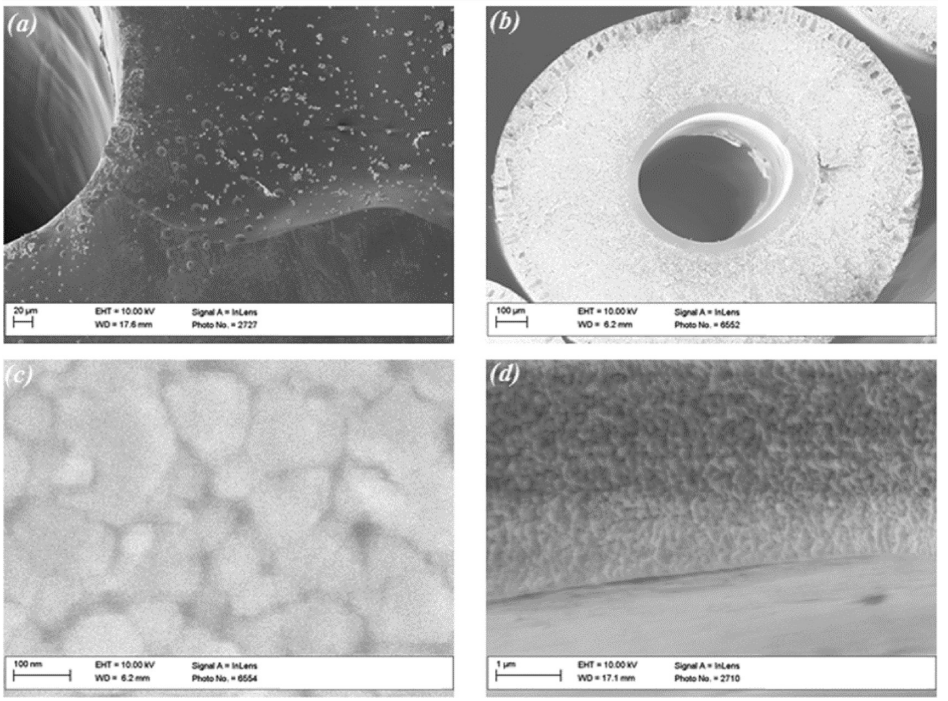

Figure 13. SEM of PVDC-coated fiber sorbents dried using the "wet" drying mode. (a) Fiber face showing smooth PVDC without any visible cracks from drying. (b) PVDC-coated fiber sorbent. (c) High-magnification of PVDC lumen layer from aged latex, showing poor particle coalescence. (d) High-magnification of PVDC lumen layer from fresh latex, showing poor particle coalescence.

the fiber (Figure 12a). Higher magnification reveals the PVDC particles have not even deformed or intercalated significantly for the aged latex (Figure 12c), while the new latex shows only marginal improvement in terms of particle deformation and intercalation (Figure 12d). Permeation experiments (Table 5) on fibers from the aged and new latex show a 4 order of magnitude reduction in permeance over the bare fibers, and a further reduction in permeance by using the fresh latex. However, both fibers are still four to 5 orders of magnitude away from a defect free layer; most likely the fissures in the face of the fiber as well as the porous nature of the lumen layer are responsible for these higher-than-expected fluxes.

4.2.3.2. "Wet" Mode. The "wet" drying mode removed the fissures in the fiber faces (Figure 16a), as can be seen in Figure 13. However, under further magnification, poor film formation is still observed for the aged latex. Partial particle deformation is observed (Figure 13c), but complete coalescence into a film is still clearly unsuccessful. SEM images also show that film cast from the fresh latex suffers from similar issues with particle deformation and intercalation (Figure 13d).

Permeation results (Table 5) reveal that the aged latex barrier layer is defective, with a helium permeance of 6.8 GPU, whereas the fresh latex barrier layer has helium fluxes at 1.45 GPU, which cannot readily be inferred via SEM images. Most likely, the fresh PVDC particles coalesce slightly better than the aged particles, resulting in a less porous lumen layer. Unfortunately, despite the marked improvement over the "dry" mode, even the fresh latex barrier layers dried in the "wet" mode are still much too defective for use in an actual RTSA operation with zeolite 13X as the CO_2 sorbent.

4.2.3.3. "Graded" Drying. The "graded" drying mode proved to be much more promising. SEM images reveal no fissures in the faces of the fiber, and upon further magnification, the aged latex exhibits highly deformed particles, but still under-developed particle−particle intercalation (Figure 14a,b) is seen throughout the PVDC lumen layer. Interestingly, the fresh PVDC lumen layer exhibits poor particle merging and intercalation throughout the bulk of the lumen layer (Figure 14c), yet the innermost radius of the lumen layer was found to have a "gradient" of particle deformation: the particles closest to the innermost radius deformed and intercalated the most, resulting in a very thin (∼50 nm) PVDC skin layer. Permeation results are the most telling (Table 5), as the fibers with the PVDC lumen layer from the aged latex formed under "graded" drying exhibit a factor of 2 decrease in permeace over the "wet" mode, reducing the helium permeance to approximately 3.3 GPUs. Finally, fresh PVDC dried with the "graded" mode yielded low helium permeances (0.21 GPU), indicating again that fresh latex and reasonably slow drying conditions are required to create a dense layer. However, the layer is still partially defective, as the selectivity through the layer is only marginally above Knudsen selectivity.

4.2.4. Toluene-Assisted Drying of Nascent PVDC Barrier Layer. The previous section showed that when using fresh latex and "graded" drying, low permeances were obtained, and SEM images showed the presence of a thin skin PVDC layer that was found to be slightly defective via permeation experiments. However, although the results presented above are encouraging, another method was devised to allow for even lower fluxes through the lumen-side barrier layer and that perhaps circumvents the main limitation of casting a latex dispersion onto a porous support. A large column of toluene was added to the top of the water column that humidified the nitrogen stream for the "graded" drying mode. Toluene was chosen because of its immiscibility with water, thereby allowing the nitrogen to be saturated in both water and toluene. Furthermore, toluene was

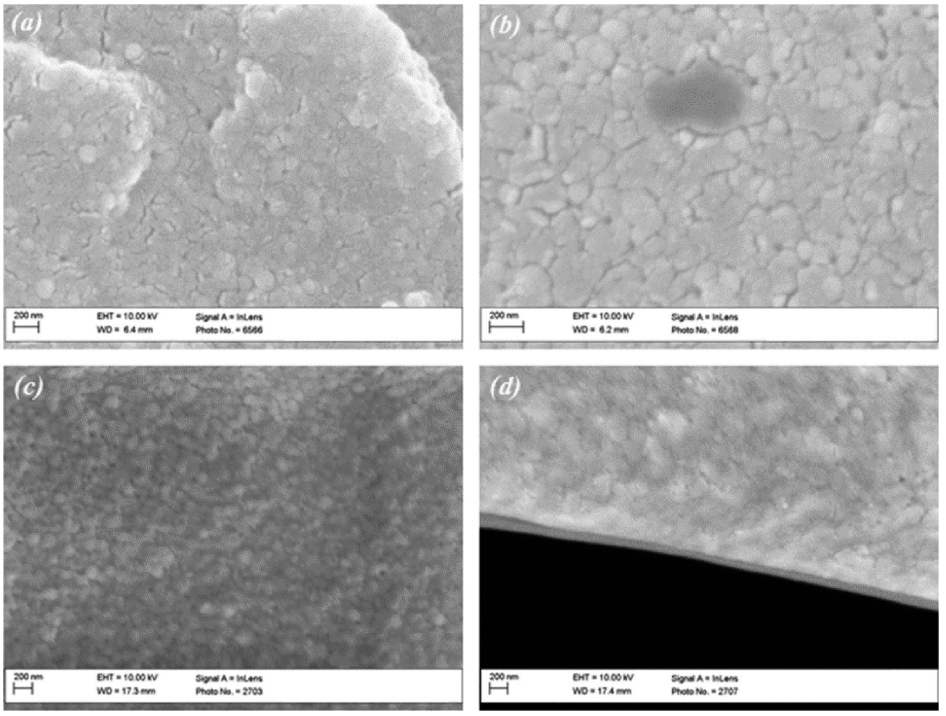

Figure 14. High-magnification SEM images of PVDC lumen layer made with "graded' drying mode. (a) PVDC lumen layer from aged latex, showing good particle deformation, but poor intercalation. (b) Higher-magnification image showing poor intercalation in aged latex film. (c) Middle of the PVDC lumen layer from fresh latex showing poor particle deformation and intercalation. (d) High-magnification image of innermost radius of the PVDC lumen layer from the fresh latex showing a continuous thin skin.

chosen because of the fact that is a known swelling solvent for PVDC.[30] As discussed in the next section, the reasoning behind this is that by controllably softening the PVDC particles with toluene, particle deformation can occur at lower pressures, thereby allowing the lumen layer to form a dense, continuous layer. As can be seen in SEM images in Figure 15, a dense, apparently defect-free skin layer has been formed with the toluene-assisted drying mode for both the aged and fresh latex. Helium permeation confirms the SEM images, as the flux is immeasurably low (<0.03 GPU) on the isobaric systems. The reliable limits of measurement in the isobaric permeation system are ~0.01−0.03 GPUs, and these fibers are most likely less permeable than that. Ideally, installing these fibers into an isochoric system would yield the actual permeance. However, because of the fact that the end-caps of the fibers must be perfect as well as the lumen layer, Swagelok fittings are avoided when working with these fiber modules (normal Swagelok fittings were found to destroy the end-caps as confirmed by SEM and permeation), and Ultratorr fittings are used in lieu of the standard fittings in the isobaric system. Unfortunately, Ultratorr fittings are not "leak-proof" enough to be used in the high-vacuum isochoric systems, and ultimately the leak-rate in the isochoric system was all that could be detected. Water permeation experiments on the toluene-assisted PVDC coated fiber sorbents revealed no water permeation through the layer at 25 °C after 5 days.

These promising results seem to indicate a path forward for creating defect-free layers on porous supports. By using a toluene drying atmosphere, at least an order of magnitude reduction in helium permeance was seen on the lumen layers cast from the fresh latex, whereas a 2 orders of magnitude reduction in helium permeance was observed in the lumen layers cast from the aged latex. In fact, the modules cast from aged latex and fresh latex were indistinguishable in terms of helium and water permeance. Though we have not explored this option, addition of toluene vapor to the other drying methods may well reduce or eliminate the differences between the aged and fresh latex, though it is unlikely that the toluene vapor will sufficiently repair large stress fractures that occur because of overly rapid drying.

5. DISCUSSION

The preceding sections described an experimental investigation of the barrier properties of films cast from aged and new PVDC latex dispersions onto porous substrates of varying character while drying the nascent films at three different rates. Though the literature discusses in detail film formation theories onto ideal substrates (there are at least two large review papers on the topic),[13,24] there are very few proposals as to how latex films form when cast onto porous substrates.[9,10] The current consensus on how latex films form on ideal surfaces can be summarized as a shrinking meniscus during drying that collects and orders the disperse PVDC particles, followed by large interfacial tension forces between the air and the evaporating water that lead to particle deformation and finally polymer−polymer interdiffusion.

As was abundantly clear in the preceding section, the drying rate of the latex must be sufficiently slow to allow for a continuous, albeit porous, film to form (as opposed to a highly cracked or crazed film). Any form of dry convective sweep or vacuum drying will rapidly pull the interstitial water out of the latex. While this forms apparently dense sections throughout the

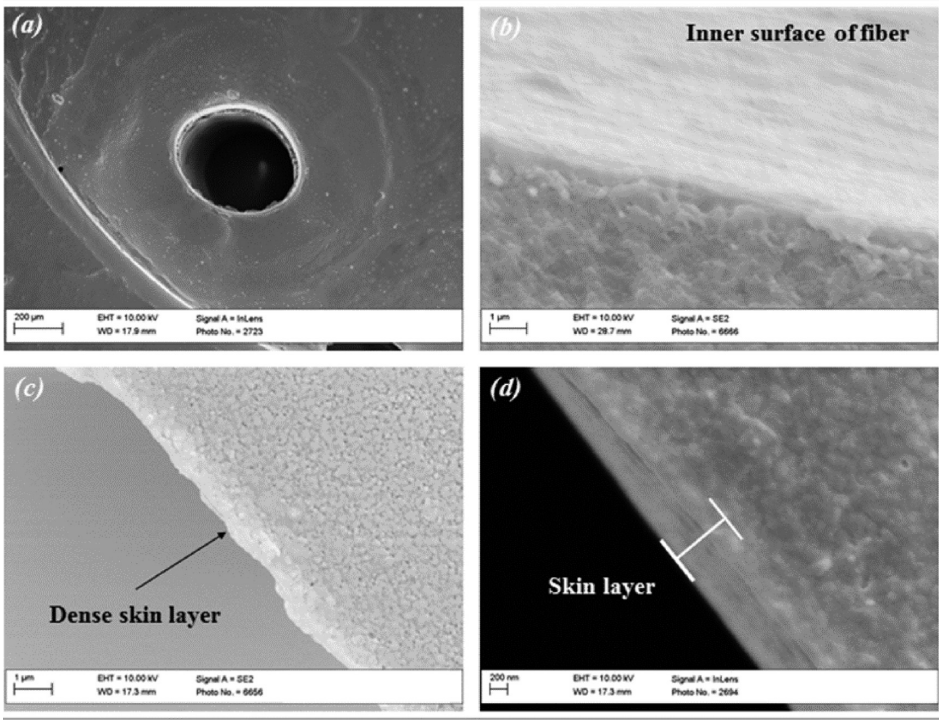

Figure 15. SEM images of PVDC-coated fibers that were dried using toluene, water vapor and nitrogen ("toluene-assisted graded drying mode"). (a) Fiber face showing smooth, crack-free PVDC coating. (b) Magnification of aged latex PVDC lumen layer showing cross-section of skin layer as well as the inner surface of the fiber. (c) SEM image of aged PVDC lumen layer clearly showing a dense skin. (d) High-magnification SEM image of fresh PVDC lumen layer showing a thick (300−500 nm) skin layer.

film (via SEM, Figure 5), the rapid film formation provides too much stress for the rapidly solidifying film, thereby causing stress-relief fractures. In the fibers, the cylindrical substrate most likely mitigates these stress-relief fractures to some extent, but on the faces of the fibers—which are equally crucial to barrier layer performance due to lumen layer bypass—the same stress-relief fractures can occur. Only in the "graded" drying mode (or the expanded toluene-assisted graded drying mode) is the nascent latex given enough time to sufficiently relax out the stresses that occur as a result of film formation. An unexpected observation was the discrepancy between the fluxes of the fibers and films dried in the "graded" mode (helium permeances of 0.21 GPU for the fiber and 5.6 GPU for the film). A very preliminary explanation is that the hydraulic pressure present in the fiber post-treatment promotes more particle deformation, whereas the films are cast without any external pressure head.

The effect of the substrate is a much more nebulous factor in the film formation process. The smooth glass substrate was used as a control, and as expected, the PVDC film (from the fresh latex) was found to coalesce into a dense, continuous structure much as the literature predicts.[13,19,31] As discussed in section 4.1.2, PVDC laticies cast onto the hydrophobic polycarbonate substrate were completely defective. In this hydrophobic case, capillary forces are thwarted by the inability of the PVDC latex to wet the surface. The areas where the PVDC beads up likely form continuous dense films, as the hydrophobic substrate acts much like a smooth glass substrate. However, as the latex does not continuously coat the substrate mask because of the lack of wetting, the permeance data simply reflect the flux through the porous substrate.

The porous, hydrophilic nylon 6,6 and cellulose acetate/13X supports yielded the most puzzling results. While the formed films appeared dense, albeit with a globular morphology, the permeation results indicate a film that is between 100 and 1000× more defective than the control films cast on the ideal substrates. Most likely, the hydrophilic porous substrate exhibits strong capillary action (Figure 16a), which pulls a large portion of the latex serum through the substrate. As a result, the evaporating-meniscus-driven ordering that occurs in the control film likely does not occur to the same extent on the hydrophilic porous substrates (Figure 16b). This reduction in particle mobility would have the effect of "flash vitrification" of the particles in place after the latex has been cast onto the substrate. Without the particles being packed closely together via a slowly shrinking/receding meniscus, the interfacial tension between the air and interstitial water will be much lower compared to the control films (Figure 16c). In the extreme case, the particles will not undergo deformation, but instead will only undergo polymer interdiffusion at the points where the particles are touching (Figure 16d). The toluene-assisted drying softens the polymer particles during the interfacial tension-induced particle deformation step, allowing for particle deformation to occur even at lower pressures.

Finally, the latex age plays a dramatic role in the film formation. The hypothesis established in the above discussion still holds. The aged PVDC clearly develops crystallinity over time as evidenced by XRD and DSC, and most likely loses a volatile leveling agent over time as well. As a result, the polymer particles will have a higher T_g than the fresh latex particles, significantly reducing the ability of the particles to deform and reducing polymer−polymer interdiffusion. This lack of particle deformation and intercalation as a result of the additional crystallinity and the rapid particle agglomeration results in a porous film that is also extremely brittle. Interestingly enough,

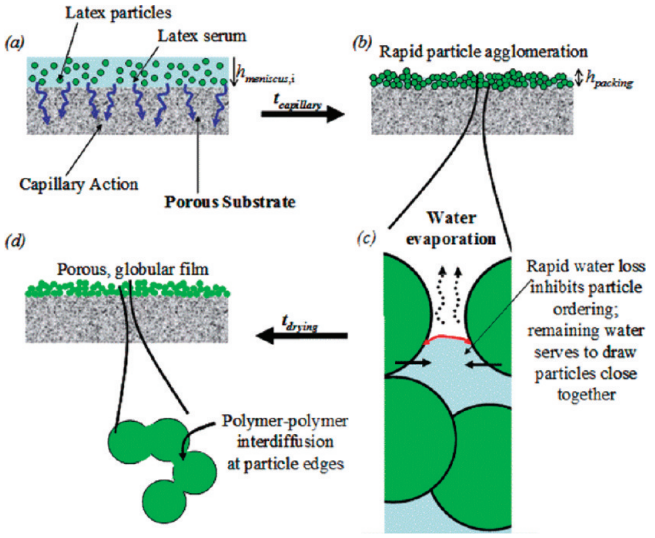

Figure 16. Schematic hypothesizing a film formation mechanism when a latex dispersion is cast onto a porous, hydrophilic substrate.

the toluene-assisted drying softens the particles enough to allow for normal particle deformation and interdiffusion to occur, as evidenced by the formation of a skin layer and the very low helium permeances.

The toluene-assisted drying method is especially promising not only for casting a lumen layer onto a fiber sorbent, but also for creating defect-free latex-based films on other porous supports. The most prominent features of this technique, that should likely be carried forward to other supports, are the slow serum evaporation rate during drying (as rapid drying often results in large stress fractures) and the use of a swelling solvent atmosphere to circumvent the "flash vitrification" effect that is observed when latexes are cast onto porous supports. Although a toluene saturated atmosphere was found to be effective in the experiments presented here, extension to other systems will likely require tuning of the drying atmosphere to ensure formation of a defect-free film. Specifically, sweep gas water concentration (for an aqueous latex), sweep gas solvent choice, sweep gas solvent concentration, drying time, and temperature need to be tailored to each individual system. The research in this paper focused primarily on forming a defect-free lumen layer within fiber sorbents, and thusly used long drying/swelling times and slow drying rates in order to successfully fabricate these layers. As efforts toward scalability are made, more rapid drying rates will be desirable; however, a balance must be struck, as it is unlikely that the swelling solvent assisted drying technique can remove large stress-fracture defects.

6. CONCLUSIONS

This study established basic guidelines and principles for creating defect-free lumen side barrier layers on fiber sorbents. Film experiments were performed in support of this goal, with the effect of drying rate, substrate hydrophobicity, substrate porosity (porous versus nonporous), and latex age being studied via film casting observations, SEM images, and helium/nitrogen permeation experiments, as well as DSC and XRD experiments. The main findings are that capillary forces in the hydrophilic cellulose acetate/13X matrix quickly dehydrate the nascent PVDC film, locking the particles in place much farther apart relative to a film cast on an ideal substrate. This additional spacing between the particles reduces the interfacial forces which causes less particle deformation—less particle deformation implies less polymer−polymer interdiffusion is occurring, resulting in a defective film. A drying method utilizing toluene as a swelling agent was utilized to soften the PVDC particles to compensate for the reduction in interfacial forces, thus allowing for a defect-free skin to be formed on the lumen side barrier layer.

■ ASSOCIATED CONTENT

Supporting Information. This material is available free of charge via the Internet at http://pubs.acs.org.

■ AUTHOR INFORMATION

Corresponding Author

*Tel.: +1 404 385 4717.Fax: +1 404 385 2683. E-mail: ryan.lively@chbe.gatech.edu.

■ ACKNOWLEDGMENT

The authors thank ExxonMobil Corporation for funding this research. W.J.K. thanks King Abdullah University for Science and Technology (KAUST) for funding his time.

■ REFERENCES

(1) Anderegg, W. R. L.; Drall, J. W., Schneider, S. H. *Proc. Natl. Acad. Sci. U. S. A.*, April 9, **2010**.
(2) Climate Change and Society Governance. *The Professional Geologist*; March **2010**, p 33.
(3) Holtz-Eaken, D.; Selden, T. M. *J. Public Econ.* **1995**, *57* (1), 85–101.
(4) *Annual Energy Outlook 2010*; Report # DOE/EIA-0383; Energy Information Administration: Washington, D.C., May 11, 2010.
(5) Pacala, S.; Socolow, R. *Science* **2004**, *305*, 968–972.
(6) Lively, R. P.; Chance, R. R.; Kelley, B.T.; Deckman, H. W.; Drese, J. H.; Jones, C. W.; Koros, W. J. *Ind. Eng. Chem. Res.* **2009**, *48* (15), 7314–7324.
(7) Lively, R. P.; Chance, R. R.; Koros, W. J. *Ind. Eng. Chem. Res.* **2010**, *49* (16), 7550–7562.
(8) Lively, R. P.; Leta, D. P.; DeRites, B. A.; Chance, R. R.; Koros, W. J. *Chem. Eng. J.* **2011**, *171* (3), 801–810.
(9) Pan, S. X.; Davis, H. T.; Scriven, L. E. *Coatings, Conference Proceedings*, TAPPI Press, Atlanta, GA, 1996, 115−133.
(10) Cairncross, R. A. *IS & TS 50th Annual Conference*, 1997, 554-558.
(11) McKelvey, S. A.; Clausi, D. T.; Koros, W. J. *J. Membr. Sci.* **1997**, *124* (2), 223–232.
(12) Padget, J. C. *J. Coat. Tech.* **1994**, *66* (839), 89–103.
(13) Keddie, J. L. *Mater. Sci. Eng.* **1997**, *21*, 101–170.
(14) Everett, D. H. *Basic Principles of Colloid Science*; Royal Society of Chemistry: Cambridge, U.K., 1998.
(15) Vanderhoff, J. W.; Bradford, E. B.; Carrington, W. K. *J. Polym. Sci.: Polym. Symp.* **1973**, *41* (1), 155–174.
(16) Sheetz, D. P. *J. Appl. Polym. Sci.* **1965**, *9* (11), 3759–3773.
(17) Brown, G. L. *J. Polym. Sci.* **1956**, *22* (102), 423–434.
(18) Rousseau, R. W. *Handbook of Separation Process Technology*; John Wiley& Sons: New York; p 917.
(19) Wang, Y.; Kats, A.; Juhue, D.; Winnik, M. A.; Shivers, R. R.; Dinsdale, C. J. *Langmuir* **1992**, *8* (5), 1435–1442.
(20) Ahareni, S. M. *J. Appl. Polym. Sci.* **1979**, *23* (1), 223–228.
(21) Sweeting, O. J. *The Science and Technology of Polymer Films*; John Wiley & Sons, Inc.: New York, 1971.

(22) Moore, T. Effects of Materials, Processing, and Operating Conditions on the Morphology of Gas Transport Properties of Mixed Matrix membranes. *PhD Dissertation*, University of Texas, Austin, TX, 2004.
(23) Moore, T.; Damle, S.; Williams, P.; Koros, W. J. *J. Membr. Sci.* **2004**, *245* (1−2), 227–231.
(24) Steward, P. A.; Hearn, J.; Wilkinson, M. C. *Adv. Colloid & Interfacial Sci.* **2000**, *86*, 195–267.
(25) Bieleman, J.; Hajas, J.; Dören, K. Flow-Levelling and Coalescing Agents. In *Additives for Coatings*; Bieleman, J., Ed.; Wiley-VCH Verlag GmbH,: Weinheim, Germany, 2007.
(26) Bragg, W. L. *Proc. Cambridge Philos. Soc.* **1913**, *17*, 43–57.
(27) Farrow, G. *Polymer* **1961**, *2*, 409–417.
(28) Schiers, J. *Compositional and Failure Analysis of Polymers: A Practical Approach*; John Wiley & Sons, New York, 2000; pp 122−123.
(29) McKelvey, S. A. Formation and characterization of hollow fiber membranes for gas separation (fiber breaks, macrovoids). *Ph.D. Dissertation*, University of Texas, Austin, TX, 1997.
(30) Osborn, K. R.; Jenkins, W. A. *Plastic Films Technology & Packaging Applications*; CRC Press: Boca Raton, FL, 1992; pp 98−99.
(31) Chevalier, Y.; Pichot, C.; Grailat, C.; Junnicot, M.; Wang, K.; Maquet, J.; Lindner, P.; Cabone, B. *Colloid Polym. Sci.* **1992**, *270* (8), 806–821.